CHAPTER 6. THRUST FORCE, TORQUE, AND TOOL WEAR IN DRILLING THE BULK METALLIC GLASS

6.1. Introduction

This study extends the previous research on drilling of BMG to the investigation of drilling thrust force, torque and drill wear [1]. Thrust force and torque are two important process parameters the drilling process. Thrust force and torque determines the energy required for chip generation. In addition, effects of tool wear, drilling process parameters (feed rate and spindle speed), plowing in the drill center chisel edge and chip generation in the main cutting edge, and tool- and work-materials can be revealed by analyzing the change in thrust force and torque. In this study, BMG and 304 stainless steel (SS304) are drilled under the same process conditions and the measured thrust force and torque are compared.

The tool wear has a strong effect on the hole quality and dimensional accuracy during drilling. The tool wear can reach a threshold level, which causes the catastrophic failure of the drill. Excess tool wear causes high forces and can damage the part, fixture, and machine tool [2]. For BMG, the low thermal conductivity facilitates high chip temperatures, which may trigger rapid exothermic oxidation of the chip and light emission during drilling [1,3]. Infrared thermometry shows that the chip flash temperature is high, in the 2400 to 2700 K range. Unlike lathe turning, the chip in drilling is constrained within narrow flutes and makes constant contact with the drill and workpiece. High temperature chip is expected to damage the drill catastrophically. Such phenomenon is revealed in this study.

One of the goals of this study is to identify feasible BMG drilling process parameters that do not generate the chip light emission and can drill multiple holes with no significant tool wear. Identification of the tool wear mechanisms, such as the flank, crater, and margin wear on the drill, and comparing with drilling of SS304 are performed. The cutting force and tool wear in lathe turning of BMG has been investigated [4].

In this paper, the experimental setup and design are first introduced. The thrust force, torque, and severe tool wear of BMG drilling with chip light-emission are analyzed. For the BMG drilling without chip light emission, the same analysis procedure is applied to analyze the thrust force and torque. Finally, progressive tool wear for drilling BMG is presented.

6.2. Experimental Setup and Design

6.2.1. Drilling test setup and measurements

The drilling experimental setup has been discussed in detail in Ref. [1]. The thrust force and torque were measured using a piezoelectric dynamometer, Kiestler 9272A. Two drill tool-materials, M7 high speed steel (HSS) and WC in cobalt matrix, denoted as WC-Co, were used. The WC-Co is 50% harder and has almost 4 times higher thermal conductivity than the HSS. A Hitachi S-4700 scanning electron microscope (SEM) was used to examine the tool wear. Prior toSEm analysis, drills were submerged in an acetone solution and cleaned using an ultrasonic cleaner to remove the adhered chips and other contaminants.

6.2.2. Experiment design

Five sets of drilling experiment, marked as Exp. I to V, were conducted. Drilling process parameters for these five sets of experiment, which are the same as those used in [1], are listed in Table 6.1. Each of the experiments has a specific goal. Effects of the feed rate, spindle speed, drill size, tool-material, and work-material are studied in Exps. I to V, respectively.

Table 6.1. BMG and SS304 drilling process parameters, light emission, the number of holes drilled, and damage on the drill.

Exp.	Work material	Drill material	Drill diameter (mm)	Feed rate (mm/min)	Spindle speed (rpm)	Light emission level [1]	Number of holes drilled	Drill severely damaged
I	BMG	HSS	1	2.5	10000	1	7	No
				5.0	10000	1	7	No
				10.0	10000	0	7	No
II	BMG	HSS	1	1.25	2500	1	3	No
				1.25	5000	2	3	Yes
				1.25	10000	2	3	Yes
III	BMG	HSS	2	2.5	10000	3	2†	Yes
				10.0	10000	3	4	Yes
IV	BMG	WC-Co	1	2.5	10000	0	7	No
				5.0	10000	0	7	No
				10.0	10000	0	7	No
V	SS304	HSS	1	2.5	10000	0	7	No
				5.0	10000	0	4‡	Yes
				10.0	10000	0	2‡	Yes
		WC-Co	1	2.5	10000	0	7	No
				5.0	10000	0	7	No
				10.0	10000	0	7	No

[1] Sparking level -- 0: No spark, 1: sparsely sparking, 2: periodically continuous spark, 3: extensive sparking
† Failed to drill through
‡ Broken tool

6.3. Thrust Force, Torque, and Tool Wear for BMG Drilling with Light Emission

BMG drilling tests with significant light emission were studied. As shown in Table 6.1, two tests in Exp. III with 2.5 and 10 mm/min feed rate show level 3 (extensive sparking) chip light emission. Two other tests in Exp. II 5,000 and 10,000 rpm, show level 2 (occasional continuous light spark) light emission. The tool wear and associated thrust force and torque for these four tests will be analyzed.

Fig. 6.1 shows the 2 mm diameter drill after drilling four BMG holes in Exp. III at 10 mm/min feed rate. Plastic deformation of the HSS is the dominant wear pattern. The cutting edges disappeared and the drill tip was rounded.

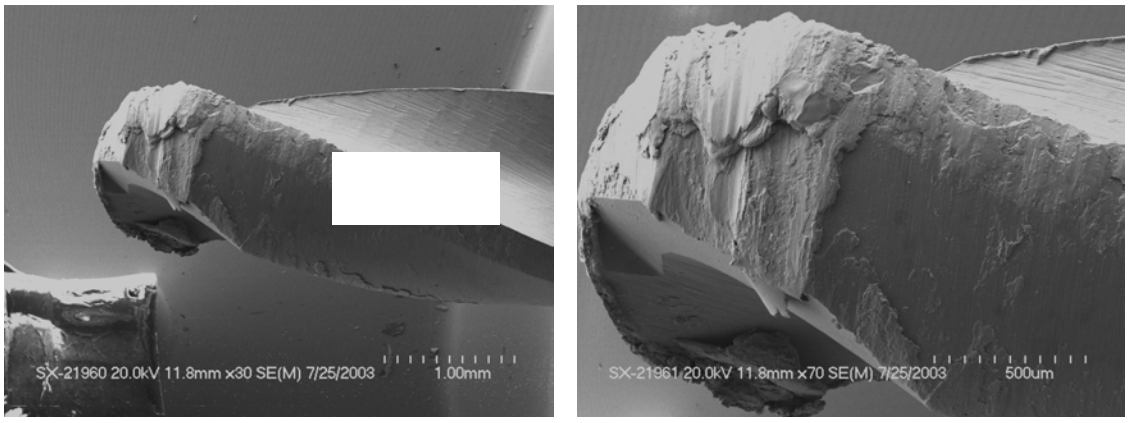

(a) (b)

Fig. 6.1. SEM micrographs of the 2 mm HSS tool in Exp. III with 10 mm/min feed rate after drilling four BMG holes: (a) overview of the drill with severe plastic deformation and the margin wear and (b) close-up view of the drill tip. (M: margin wear)

During drilling, the chip light emission was extensive. This indicates a very high chip temperature. Since the chip is constrained in the flute, high tip temperature of the drill is expected. Also, the low thermal conductivity of BMG (4 W/m-K) and HSS tool

(20 W/m-K) inhibits the transfer of heat and results in higher drill temperatures. High temperature softens the tool material and triggers large plastic deformation. Surprisingly, the worn drill was still able to penetrate the 2 mm deep BMG disk and generate holes. The shape of these holes, concomitant with large plastic deformation, has been presented in [1].

Results of the thrust force and torque vs. time, are shown in Fig. 6.2. The first two holes took about the same time (8 s) to penetrate. The last two holes took much longer, over 20 s, to break through which indicates a large amount of tool wear and plastic deformation of the workpiece.

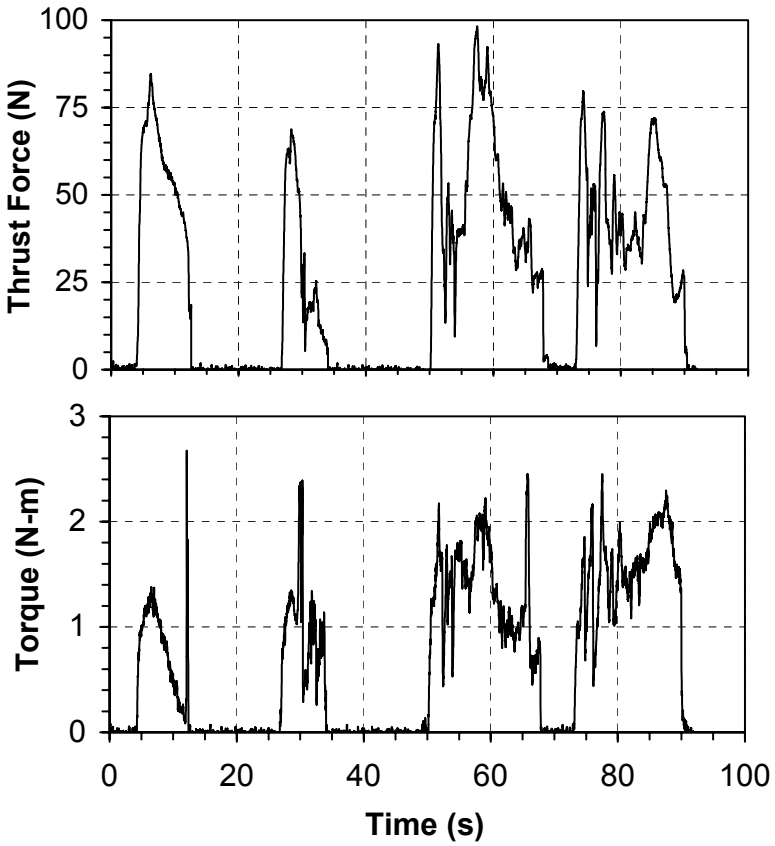

Fig. 6.2. Thrust force and torque of Exp. III at 10 mm/min feed rate: (a) thrust force and (b) torque.

Local peaks in the thrust force and torque can be observed in Fig. 6.2. Since a severely oxidized powder chip morphology was observed [1], it is likely that the clogging of the powder chips at cutting edges generates force peaks, which, in turn, further damages the drill cutting edges.

The margin wear, marked as M in Fig. 6.1(a), due to the rubbing of the drill and hole surface can be recognized on the drill margin. For the other drilling test in Exp. III (2.5 mm/min feed rate), deformation and wear of the drill are even more severe. The first hole cannot be penetrated even with the 2 mm over travel at the end of the drilling cycle. The molten BMG fills the flute of the 2 mm diameter HSS drill and makes drilling impossible. The drill did not break, but its tip was rounded and deformed to a level more severe than the drill shown in Fig. 6.1.

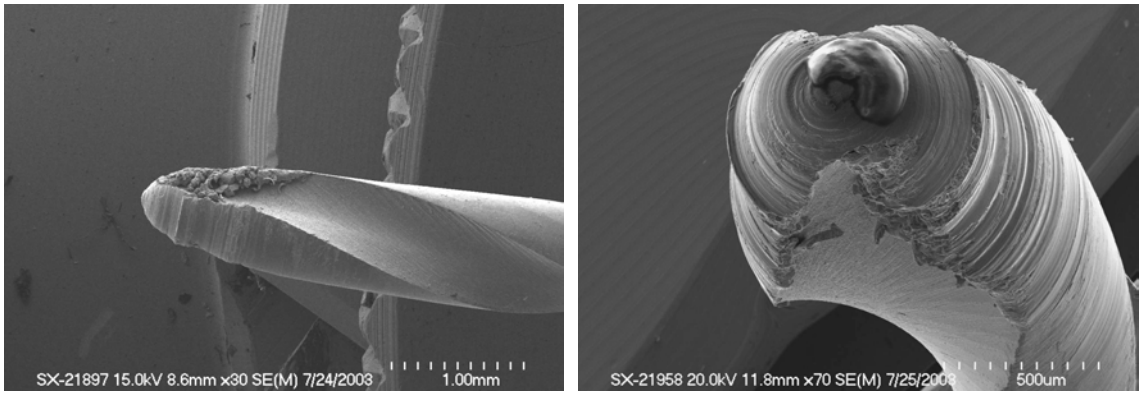

(a) (b)

Fig. 6.3. Wear of HSS drill: (a) and (b) Exp. II at 10,000 rpm spindle speed and 1.25 mm/min feed rate with periodically continuous light emission.

The other two BMG drilling tests, which have level 2 (periodically continuous) chip light emission are the two high spindle speed (5,000 and 10,000 rpm) tests in Exp. II. The severely worn drill for the 10,000 rpm test is shown in Figs. 6.3(a) and 6.3(b).

The drill tip is rounded, like the drill in Fig. 6.1. Less plastic deformation and more obvious attrition wear are seen for the drill in Exp. II, possibly due to the much lower feed rate (1.25 mm/min).

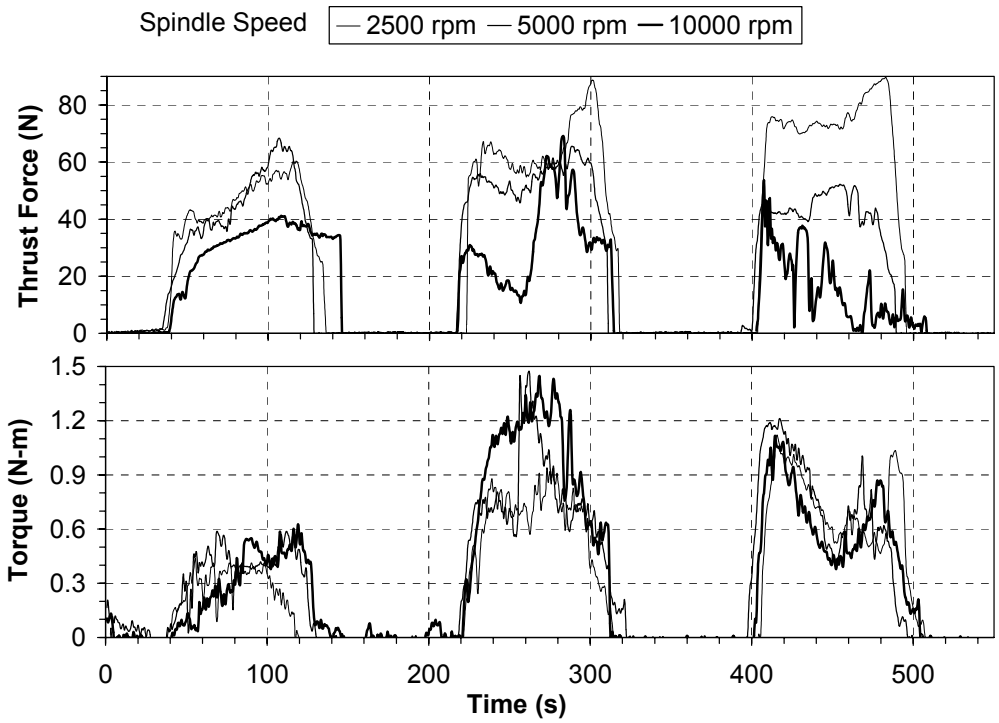

Fig. 6.4. Spindle speed effect on the thrust force and torque in Exp. II.

The thrust force and torque for drilling three holes are shown in Fig. 6.4. Lower thrust forces can generally be seen at higher speeds [5]. The effect of spindle speed on torque is not obvious. This can be explained by the very small feed per revolution in drilling the 1 mm hole using high spindle speed. The feed per revolution for the 2,500, 5,000, and 10,000 rpm spindle speed and 1.25 mm/min feed is only 0.5, 0.25, and 0.125 μm, respectively. This is much smaller than the tool edge radius. Therefore, the spindle

speed does not affect thrust force and torque significantly [6]. For the severely worn drill at 10,000 rpm, the time for drilling is expected to be longer.

Fig. 6.5 shows a 1 mm diameter HSS drill, which has been used for drilling BMG at low spindle speed (2,000 rpm) and the same 1.25 mm/min feed rate as in Exp. II. This drilling condition was presented as Exp. VII in [1]. Due to insufficient cutting speed, this drill broke during the drilling test. At low spindle speed, the work-material builds up at the cutting and margin edges, as shown in the close-up view of the cutting and margin edges in Fig. 6.5(b). This causes the large cutting forces and drill breakage.

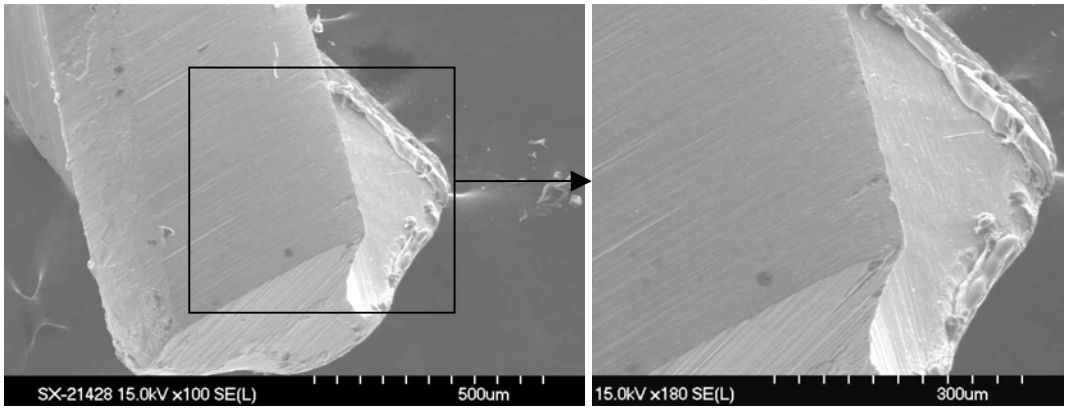

(a) (b)

Fig. 6.5. Effect of low spindle speed on the build-up work-material on the cutting and margin edges: (a) drill broke at 2,000 rpm spindle speed and 1.25 mm/min feed rate and (b) close-up view of the material build-up.

In summary, drilling BMG at high speed generates the chip light emission, high tool temperature, and severe tool wear. In contrast, drilling the BMG at low speed causes the work-material to build-up at cutting edges, produces large cutting forces, and results in the broken drill. Like drilling of other metallic materials, there is a range of feasible

spindle speed and feed rate for the efficient drilling of BMG without the light emission and material build-up.

6.4. Thrust Force and Torque for BMG Drilling with No Light Emission

Drilling of BMG without light emission and the associated thrust force and torque data and tool wear results are discussed in this section. In Exps. I and VI, seven 1 mm holes was successfully drilled on BMG without drill wear and light emission.

Fig. 6.6 shows the thrust force and torque for seven holes drilled under the same process conditions (10,000 rpm spindle speed and 5 mm/min feed rate) for BMG in Exps. I and IV and for SS304 in Exp. V. The effects of tool-material (HSS vs. WC-Co), work-material (BMG vs. SS304), and hole number can be summarized as follows:

1. *Effect of work-material*: Most notable in Fig. 6.6 is the broken HSS tool in drilling of SS304. The gradual increase of the thrust force and torque that eventually leads to the failure of the HSS drill in hole #4 can be recognized. Build-up of work-material in cutting and margin edges, similar to that observed in Fig. 6.5, is the likely cause of drill failure. Both the HSS and WC-Co tool successfully drilled seven holes on the BMG workpiece. When the process parameters are correct, drilling BMG is not difficult. Using the WC-Co tool, drilling BMG generally requires higher thrust force than that for SS304. The torque level is about the same. It can be noted that SS304, an austenitic stainless steel, is a difficult-to-drill material with a high strain hardening rate (0.6), high fracture toughness (K_{IC} of 75–100 MPa-$m^{1/2}$), low thermal

conductivity (16 W/m-K) and good ductility (40%). At 10 mm/min feed rate in Exp. V, the HSS drill broke in the second hole. In this regard, the BMG, when the process conditions are right, is easier to drill than SS304.

2. *Effect of tool-material*: An HSS drill generally has higher force and about the same torque compared to a WC-Co drill. A large portion of thrust force, over 50%, is contributed by the plowing in the drill center chisel edge [7]. The harder WC-Co drill has a higher elastic modulus and produces less wear and deformation in the drill chisel edges. This leads to more efficient plowing of the work-material compared to the HSS tool.

3. *Effect of hole number*: The thrust force and torque both changes from hole to hole. For BMG drilling using the HSS tool, the thrust force and torque both gradually increase and then decrease from the first to the seventh hole. The trend is different for drilling BMG using the WC-Co tool. The thrust force stays at the same level and the torque gradually increases and, like the thrust force, reaches a steady level after hole #3. For SS304 drilled by WC-Co, the thrust force gradually decreases and the torque remains at about the same level after the third hole. This variation of thrust force and torque is further studied by extracting representative values from the data of each hole drilled.

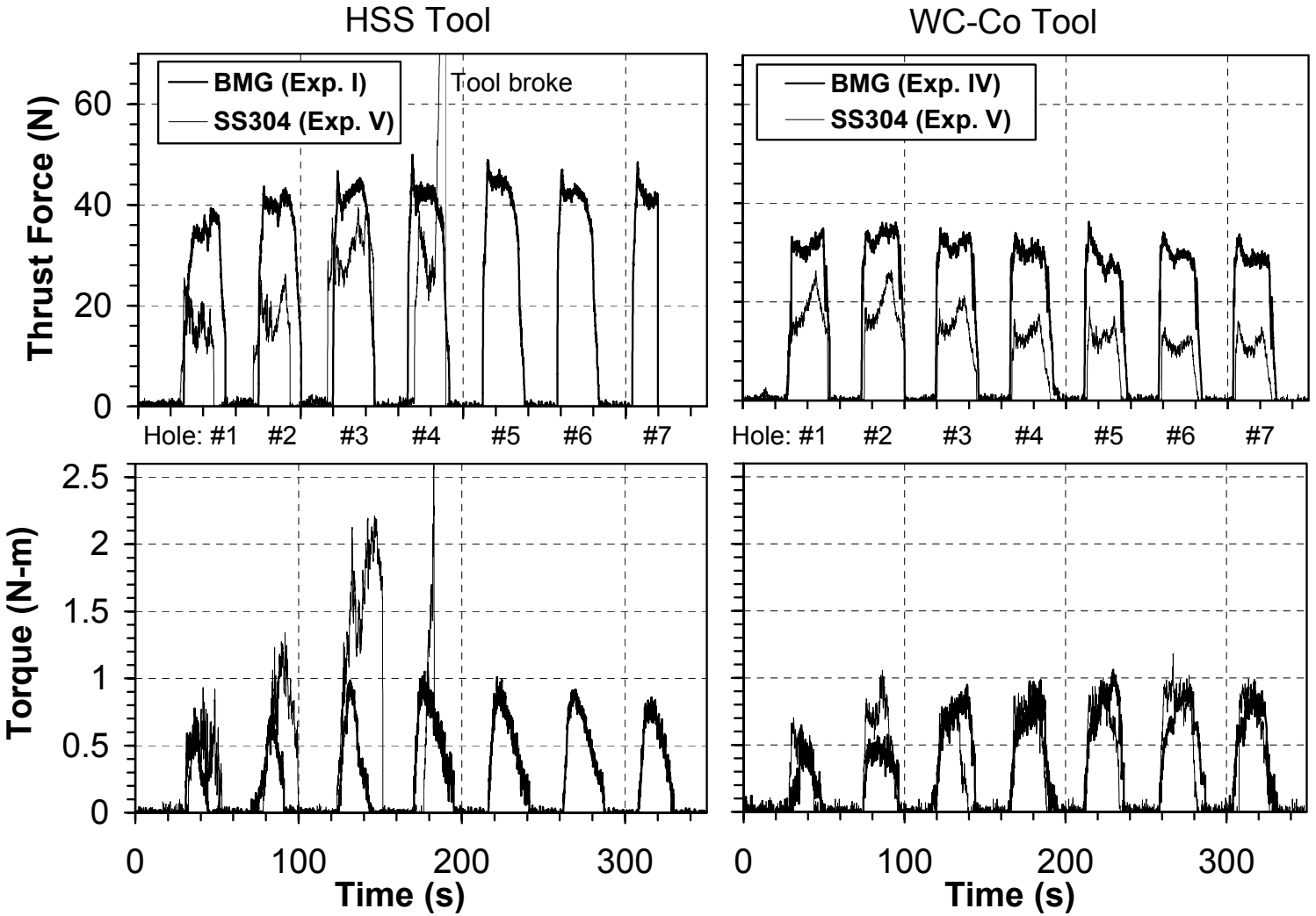

Fig. 6.6 Effects of work-material, tool-material, and hole number for drilling BMG and SS304 at 5 mm/min and 10,000 rpm (Exps. I, IV, and V).

As shown in Fig. 6.6, the measured thrust force and torque exhibit variations vs. time. A peak thrust force may occur after the initial contact. For the torque, it gradually increases until the full engagement of the drill conical surface and workpiece occurs, as illustrated in Fig. 6.7. The rubbing of the drill margin with the hole surface and evacuation of the chip may further increase the torque slightly, as shown in the WC-Co drilling of BMG in Fig. 6.6. The thrust force and torque, at the time when the drill's conical surface is in full contact with the workpieces are used as the representative values. For the 1 mm drill with 118° point angle, the distance d shown in Fig. 6.7(a) is 0.300 mm. The time Δt required to travel this distance for the 2.5, 5, and 10 mm/min feed rate is 7.2, 3.6, 1.8 s, respectively. For each hole drilling, the time of starting contact, t_0, is first identified in the drilling thrust force and torque vs. time data. The thrust force and torque value at the time $t_0+\Delta t$ are used as the representative values for the hole.

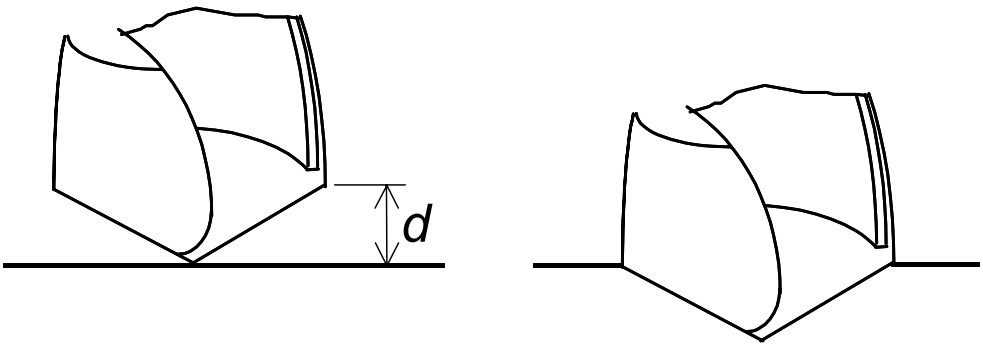

Fig. 6.7. The drill location to extract representative thrust force and torque data: (a) initial contact location and (b) full engagement of the conical drill surface and workpiece.

Fig. 6.8 summarizes the thrust force and torque for drilling seven BMG holes in Exps. I and IV. The second order polynomial trend line is used to fit the HSS BMG

drilling thrust force and torque data points (Exp. I), represented by triangular-shape symbols. The linear trend line has a better fit of the WC-Co drilling data points of thrust force and torque in Exp. IV, represented by circular shape symbol.

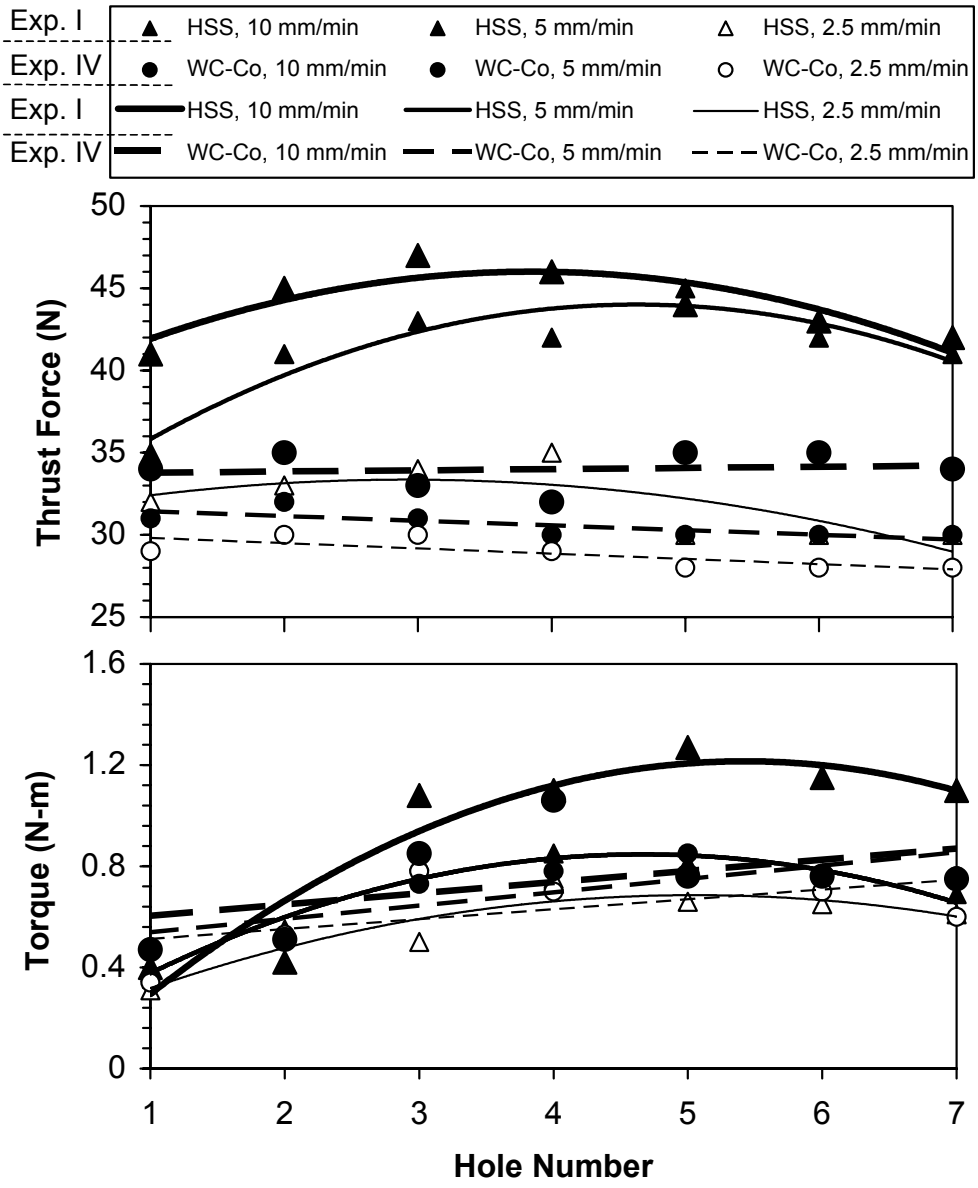

Fig. 6.8. Feed rate effect on thrust force and torque values on BMG drilling in Exp. I (solid lines) and IV (dashed lines).

For HSS, the trend of gradual increase followed by decrease of thrust force and torque for drilling the seven holes is observed of all three feed rates, 2.5, 5, and 10 mm/min. For WC-Co, the thrust force is gradually decreased and the torque is gradually increased. The wear of the cutting edges and heat accumulation at the drill cutting edge are expected to cause such changes. The initial increase in force and torque for HSS drilling of BMG is likely caused by the rapid wear of the initial sharp cutting edges [6,8,9]. Once the edges are rounded to a more stable condition, the tool temperature increases and accumulates at the drill tip, particularly for the HSS which has four times lower thermal conductivity than that of WC-Co. The high drill tip temperature changes the partition of heat at the friction interface. This increases the chip temperature, softens the work-material, and slightly decreases the thrust force and torque [2]. For WC-Co tools, the initial cutting edge rounding effect is manifest by the increasing torque in hole #2. The slight increase of torque from hole #3 to #7 can be explained by the wear of major cutting edges, particularly the region near the periphery of the drill.

6.5. Tool Wear for BMG Drilling with No Light Emission

The development of flank and margin wear for HSS drilling the BMG in Exp. I, for 5 mm/min or lower feed rate, is shown in Figs. 6.9 and 6.10, respectively. After drilling the first, third, fifth, and seventh hole, the drill is removed each time, cleaned in ultrasonic cleaner, and examined using the SEM to see the incremental tool wear.

Fig. 6.9(a) shows the new drill with sharp cutting edges. After drilling the first hole, as shown in Fig. 6.9(b), minimal flank wear is observed. In the drill center chisel

edge, residual BMG material fused on the chisel edge can be observed in Figs. 6.9(b), 6.9(c), and 6.9(d). The ultrasonic cleaning prior to SEM was not able to remove the build-up edge.

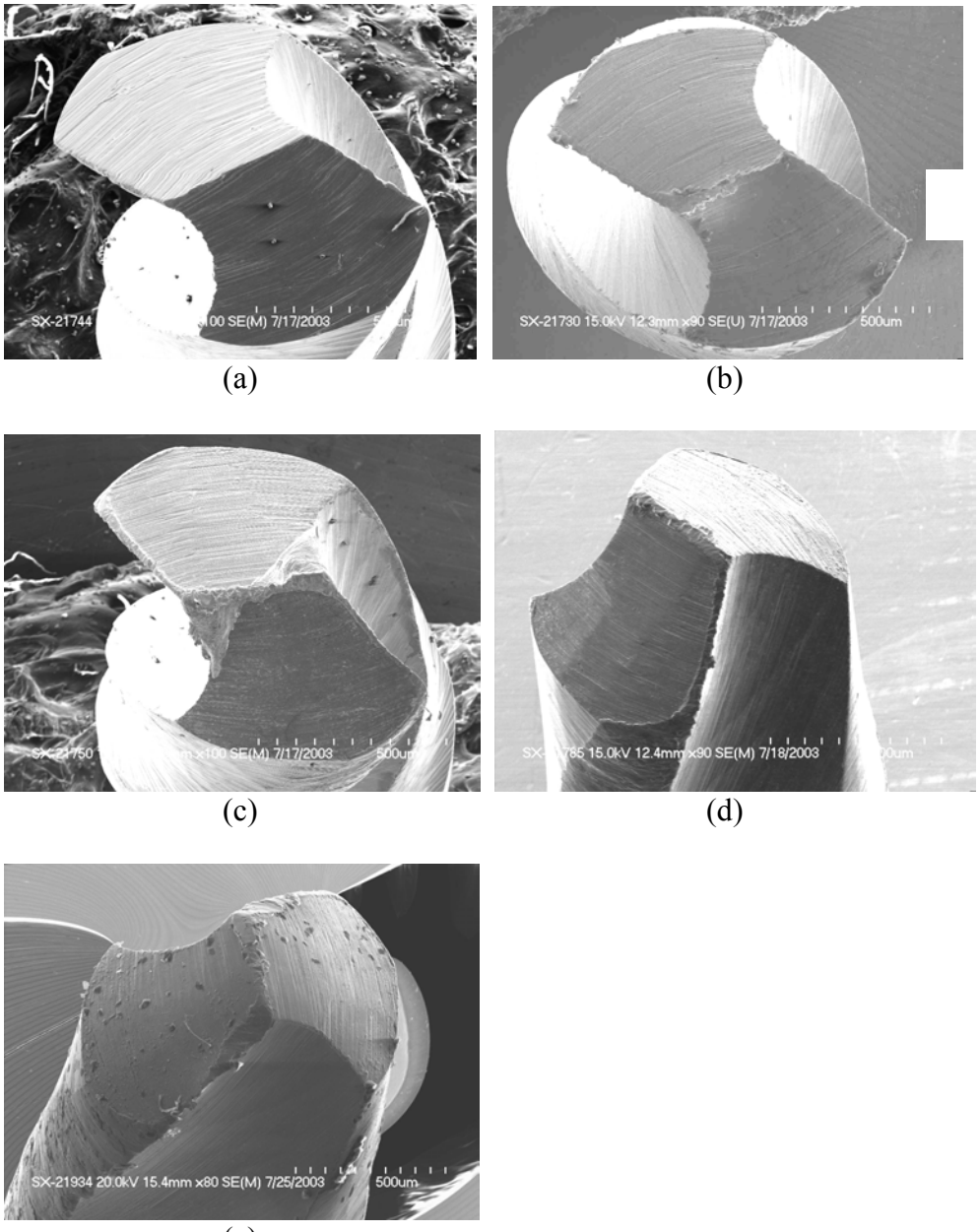

(a) (b)

(c) (d)

(e)

Fig. 6.9. Flank wear in HSS drilling of BMG (Exp. I, 5 mm/min feed rate): (a) new tool, (b) after first hole, (c) after third hole, (d) after fifth hole, and (e) after seventh hole.

As shown in Fig. 6.9(e), after drilling seven holes at 10,000 rpm and 5 mm/min, the chisel edge of the HSS drill remains in good shape with slight edge rounding. A wear land can be observed on both sides of the major cutting edge. On the two extreme ends of the major cutting edge, the negative rake angle and low cutting speed near the drill center and the high rake angle and high cutting speed near the outside corner promote flank wear [7,9]. The HSS drill is still usable after drilling seven holes on BMG.

The development of margin wear is shown in Fig. 6.10. Fig. 6.10(a) shows the margin after drilling one hole. Residual BMG on the tool tip can be observed and a side view of the margin shows about 10 μm of roll-over tool material. The width of roller-over gradually increases to about 50 μm after drilling the third and fifth holes. Fig. 6.10(d) shows the margin area and a close-up view. The margin wear on the small, 1 mm diameter drill rotating at 10,000 rpm is inevitable due to the inherent run-out of the drill with over 15 mm overhang [1]. The drill run-out will create the margin wear, as illustrated in Fig. 6.10(e).

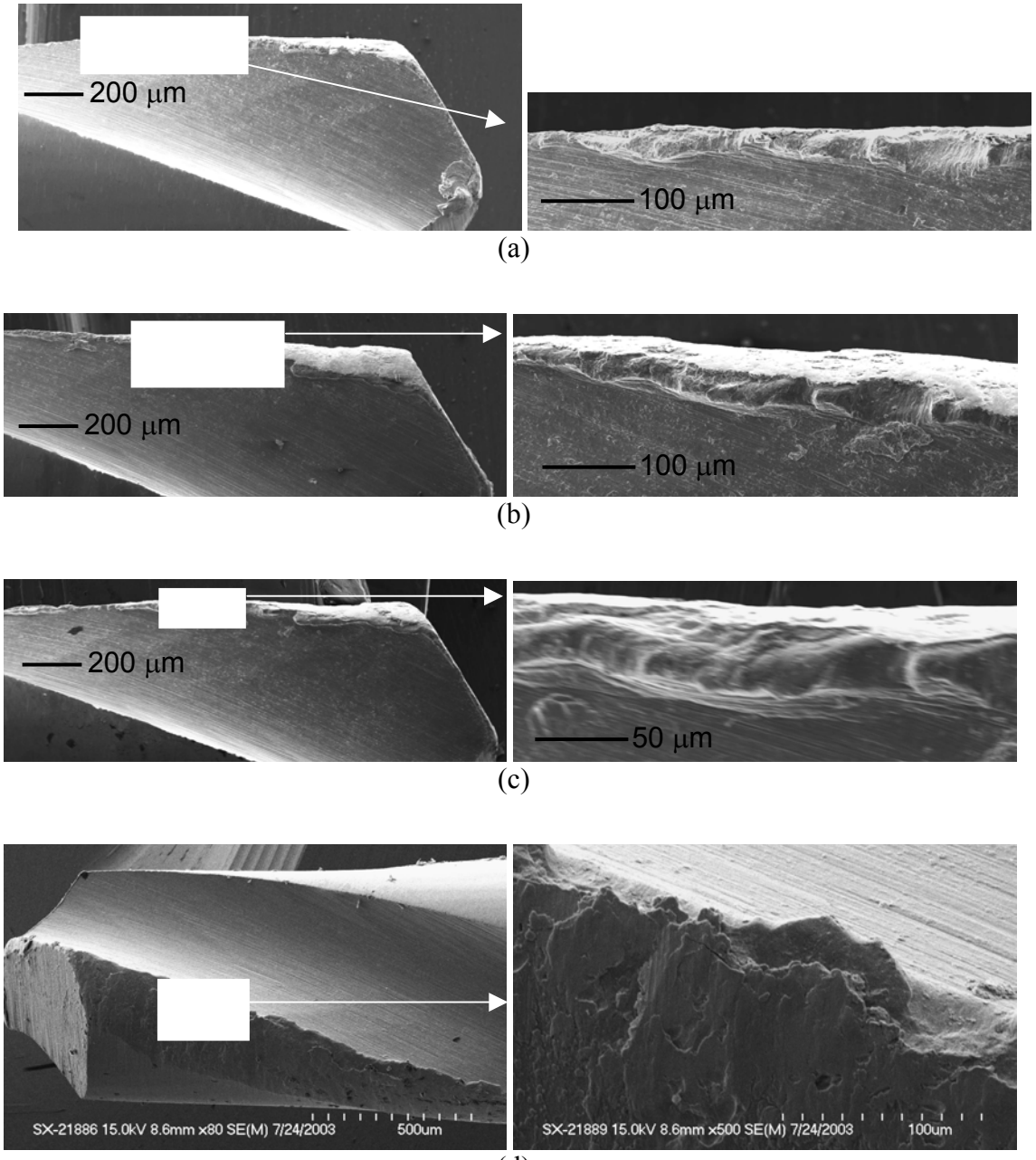

Fig. 10. Margin wear in HSS drilling of BMG (Exp. I, 5 mm/min feed rate): (a) after first hole, (b) after third hole, (c) after fifth hole, and (d) after seventh hole.

6.6. Concluding Remarks

This study showed that, when feasible process parameters are selected, BMG could be efficiently drilled using either the HSS or WC-Co tool. The WC-Co tool with better mechanical and thermal properties is the better choice for drilling BMG. The chip light emission, which is associated with high chip and tool temperatures, showed the detrimental effect on the drill life. For drilling without light emission, both HSS and WC-Co tools performed well in BMG drilling. The analysis of tool wear further confirmed such statement.

The research into machining of BMG is continuing in several fronts. The next step is the micro-milling, grinding, polishing and electrical discharge machining processes. In recent years, new Fe-, Al-, and Ti-based BMG materials have been developed. This has created the needs and opportunities for research into machining processes for precision shaping of these new, advanced engineering materials.

References

[1] Bakkal M., Shih A. J., McSpadden S. B., Scattergood R. O., "Force, torque, and tool wear in drilling of bulk metallic glass," *International Journal of Machine Tool and Manufacturing*, (submitted).

[2] Noori-Khajavi A., Komanduri R., 1995, "Frequency and time domain analyses of sensor signals in drilling - I. Correlation with drill wear," *International Journal of Machine Tools and Manufacturing*, Vol.35/6, pp. 775-793.

[3] Bakkal M., Liu C. T., Watkins T. R., Scattergood R. O., Shih A. J., 2004, "Oxidation and crystallization of Zr-based bulk metallic glass due to machining," *Intermetallic*, Vol. 12, pp. 195-204.

[4] Bakkal M., Shih A. J., Scattergood R. O., 2004, "Chip formation, cutting forces, and tool wear in turning of Zr-based bulk metallic glass," *International Journal of Machine Tool and Manufacture*, Vol.44/9, pp. 915-925.

[5] Lin S. C, Ting C. J., 1995, "Tool wear monitoring in drilling using force signals," *Wear*, Vol. 180, pp. 53-60.

[6] Guo A., Batzer S., Roth J., 2003, "Time and frequency domain investigation of the static and dynamic characteristics of micro-drilling," *Proceedings of IMECE`03, ASME International Mechanical Engineering Congress and R&D Expo,* Washington, D.C., USA.

[7] Strenkowski J. S., Hsieh C. C., Shih A. J., "An Analytical Finite Element Technique for Predicting Thrust Force and Torque in Drilling," *International Journal of Machine Tools and Manufacture,* in press.

[8] Boothroyd G., Knight W. A., 1989, *Fundamentals of machining and machine tools*, 2nd Ed., Dekker, New York.

[9] Shaw M. C., 1984, *Metal cutting principles*, Oxford.